Photoluminescence and optical absorption caused by the F^+ centres in anodic alumina membranes

2001 J. Phys.: Condens. Matter 13 2691

(http://iopscience.iop.org/0953-8984/13/11/323)

INSTITUTE OF PHYSICS PUBLISHING JOURNAL OF PHYSICS: CONDENSED MATTER

J. Phys.: Condens. Matter **13** (2001) 2691–2699 www.iop.org/Journals/cm PII: S0953-8984(01)15721-8

Photoluminescence and optical absorption caused by the F^+ centres in anodic alumina membranes

Y Li[1], G H Li[1], G W Meng[1], L D Zhang[1] and F Phillipp[2]

[1] Institute of Solid State Physics, Chinese Academy of Sciences, PO Box 1129, Hefei 230031, People's Republic of China
[2] Max-Planck-Institut fur Metallforschung, Heisenbergstrasse 1, D-70569 Stuttgart, Germany

E-mail: ghli@mail.issp.ac.cn (G H Li)

Received 14 July 2000, in final form 13 February 2001

Abstract

Anodic alumina membranes (AAMs) with highly ordered nanochannel arrays were prepared by anodizing aluminum in acid solutions. X-ray diffraction reveals the amorphous nature of AAMs. The photoluminescence (PL) excitation spectra of AAMs consist of a broad band centred at 235 nm and a narrow band peaking around 360 nm under a monitoring wavelength of 470 nm. There are five prominent absorption bands (or edges) at 370, 294, 254, 220 and 204 nm in the absorption spectra of AAMs prepared in oxalic solution. With the increase of the annealing temperature, the intensities of PL and absorption bands increase first, then decrease, and a blue-shift is found. The photoluminescence and optical absorption in the wavelength range of 200 nm to 500 nm are caused by the F^+ centres in AAMs. The energy levels of F^+ centres in AAMs are split and a new energy level of 3.35 eV appears due to the amorphous nature of AAMs.

1. Introduction

Anodic alumina membranes (AAMs) with highly ordered nanochannel arrays have been widely used as templates to prepare highly ordered nanorod/nanowire arrays [1–6]. Study of the self-properties of AAMs is important to the investigation of the mechanism of new properties that appear in the nanomaterials synthesized using AAMs as templates. However, little has been reported on the physical properties of the AAMs. Du *et al* observed a blue PL band peaking around 470 nm with a 360 nm excitation for porous alumina membranes [7]. They suggested that this blue PL band originates from the singly ionized oxygen vacancies (F^+ centres) in porous alumina membranes, but did not give a very convincing explanation. In fact, the last calculated and experimental data showed that the F^+ centre in Al_2O_3 did not exhibit the features of 360 nm excitation and 470 nm emission bands [8–13]. On the other hand, it has been found that the F^+ centre in Al_2O_3 causes a blue emission band at about 420 nm with a corresponding excitation band at about 245 nm [9–13]. Do AAMs possess similar PL properties?

0953-8984/01/112691+09$30.00

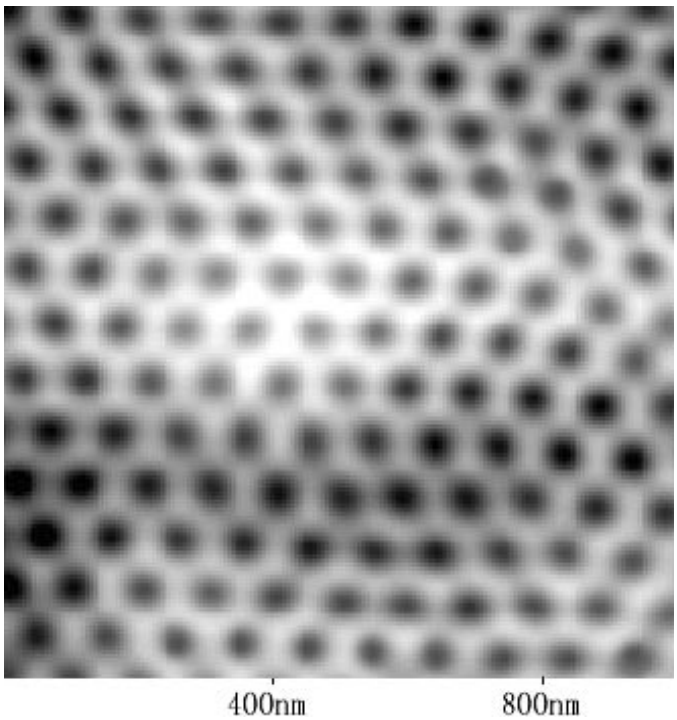

Figure 1. AFM top view image of an AAM prepared in $C_2H_2O_4$.

In addition, many spectroscopic studies have been carried out for Al_2O_3 crystals obtained by various methods, such as (1) irradiating pure Al_2O_3 with electrons [9–12, 14, 15], neutrons [16] and low-energy [17] and high-energy ions [18]; (2) using a 'subtractively coloured' method to heat Al_2O_3 in a graphite crucible under strongly reducing conditions at 2000 °C [19, 20] and (3) doping sapphire with titanium (Ti:Al_2O_3) [13]. As will be shown below, AAMs with highly ordered nanochannel arrays exhibit interesting optical properties. Research on these properties may offer a new way to explore the mechanism of the optical behaviour of Al_2O_3 crystals and give possibilities to utilize AAMs in solid-state lasers [21] and optical data storage [22]. In this paper, the photoluminescence (PL) and optical absorption properties of AAMs are investigated experimentally and the mechanism of the optical behaviours of AAMs is discussed.

2. Experiment

Two kinds of AAM with nanochannel diameters of 20 and 40 nm were prepared by using 0.3 M oxalic acid ($C_2H_2O_4$) and 0.3 M sulphuric acid (H_2SO_4) as electrolyte, respectively. The detailed anodization process has been described elsewhere [6].

After annealing the as-prepared AAMs at different temperatures for 7 h, the PL and optical absorption spectra were measured at room temperature. PL results were collected using a Hitachi model 850 fluorescence spectrophotometer with a photomultiplier R928 detector; an edge filter and a monochromator were used for monitoring PL spectra. X-ray diffraction (XRD) and electron paramagnetic resonance (EPR) measurements were also performed for AAMs annealed at different temperatures for 7 h.

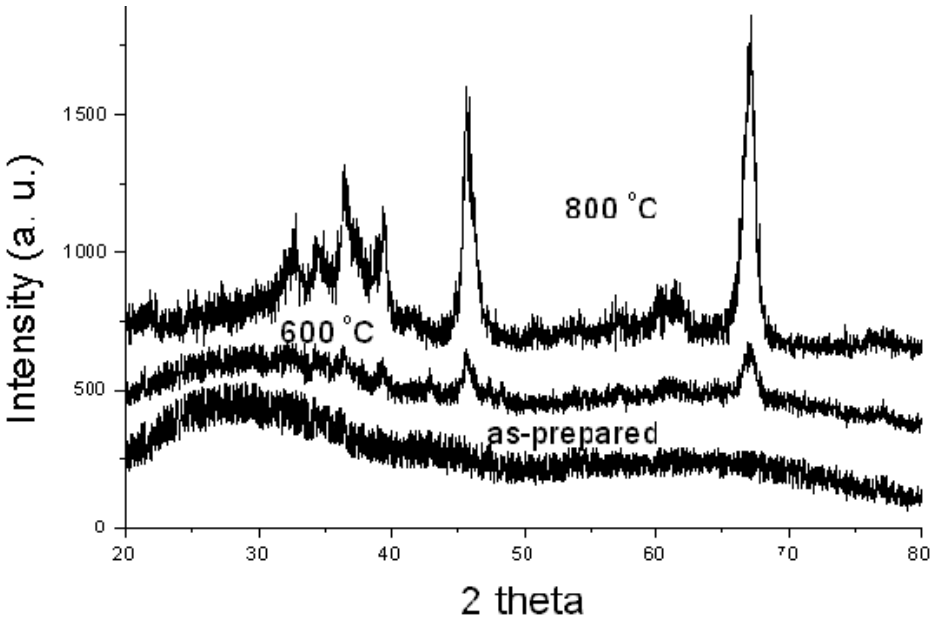

Figure 2. X-ray diffraction of AAMs prepared in $C_2H_2O_4$ after being annealed at different temperatures for 7 h.

3. Results and discussion

The AFM top view image of an AAM prepared in $C_2H_2O_4$ is shown in figure 1. The nanochannels with a narrow size distribution form almost perfect hexagonal arrays. X-ray diffraction (figure 2) verifies that the as-prepared AAMs are amorphous. It can be seen from figure 2 that the AAMs are crystallized partly after being annealed at high temperature.

Figure 3 presents the excitation spectra of AAMs prepared in $C_2H_2O_4$ (sample A) in the wavelength range of 200 nm to 400 nm. The monitoring wavelength is 470 nm and a 290 nm filter was used. A narrow excitation band peaking around 360 nm (3.44 eV) and a broad excitation band centred at 235 nm (5.28 eV) were observed. It can also be seen that, after being annealed at 600 °C, the broad band at 235 nm consists of two peaks at 220 nm (5.64 eV) and 250 nm (4.96 eV). With rising annealing temperature, the excitation spectra in figure 3 exhibit a blue-shift. Figure 4 shows the PL emission spectra with an excitation of 360 nm for sample A. With the increase of the annealing temperature T, the intensity of emission band peaking around 470 nm increases first, reaches a maximum when $T \leqslant 480\,^{\circ}$C, and then decreases. In addition, with rising T, the emission spectra in figure 4 exhibit a blue-shift. Figure 5 shows the emission spectra for sample A, with an excitation wavelength of 235 nm. When annealing temperature $T \leqslant 480\,^{\circ}$C, the emission spectra for sample A consist of a broad band with a maximum located at around 470 nm (2.64 eV). However, this band has a shoulder at 420 nm (2.95 eV). When $T \geqslant 600\,^{\circ}$C, this shoulder has a higher intensity than that of the peak at 470 nm. For AAMs prepared in H_2SO_4 (sample B), the excitation and emission spectra were measured and the similar PL phenomena were also observed. The excitation spectrum for the monitoring wavelength at 420 nm is given in figure 6 with a 290 nm filter. It should be pointed out that the bands at about 360 nm (figure 6) do not mean that the 360 nm excitation results in an emission centred at 420 nm. For the 360 nm excitation, the peak of the emission band is at 470 nm.

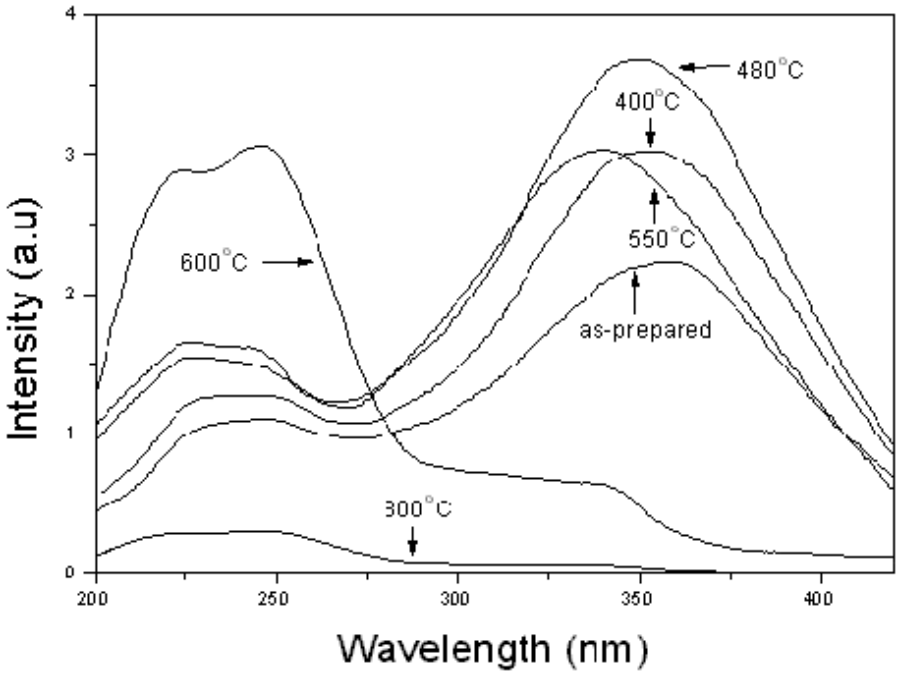

Figure 3. Excitation spectra for AAMs prepared in $C_2H_2O_4$ (sample A) after being annealed at different temperatures for 7 h. All the spectra were obtained under a monitoring wavelength of 470 nm.

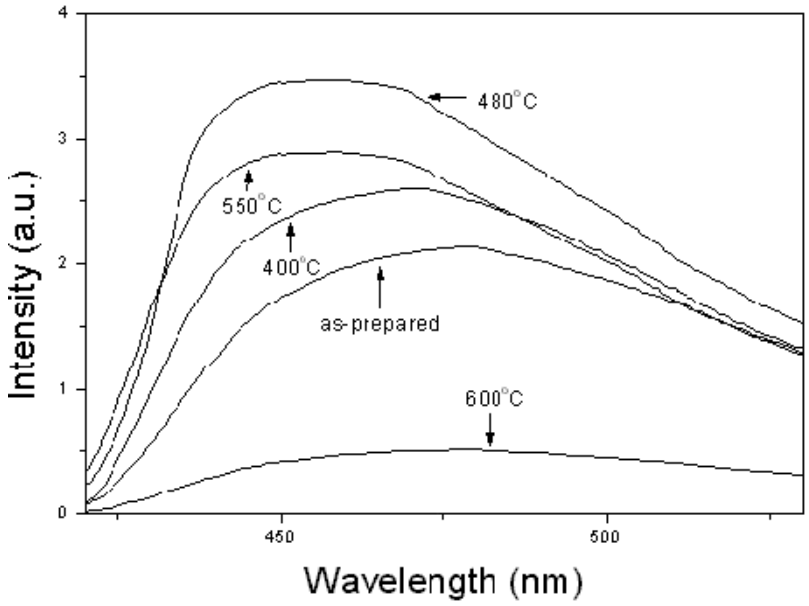

Figure 4. Emission spectra for AAMs prepared in $C_2H_2O_4$ (sample A) after being annealed at different temperatures for 7 h with an excitation wavelength of 360 nm.

The absorption spectra for sample A (figure 7) show that there are five prominent absorption bands (or edges) at 370 (3.35 eV), 294 (4.22 eV), 254 (4.88 eV), 220 (5.64 eV)

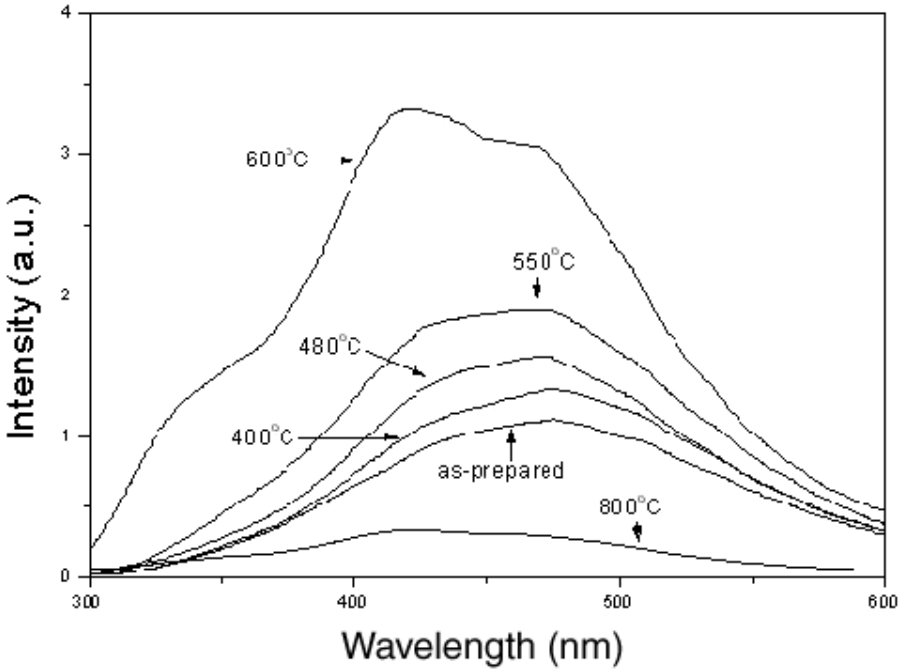

Figure 5. Emission spectra for AAMs prepared in $C_2H_2O_4$ (sample A) after being annealed at different temperatures for 7 h under 235 nm excitation.

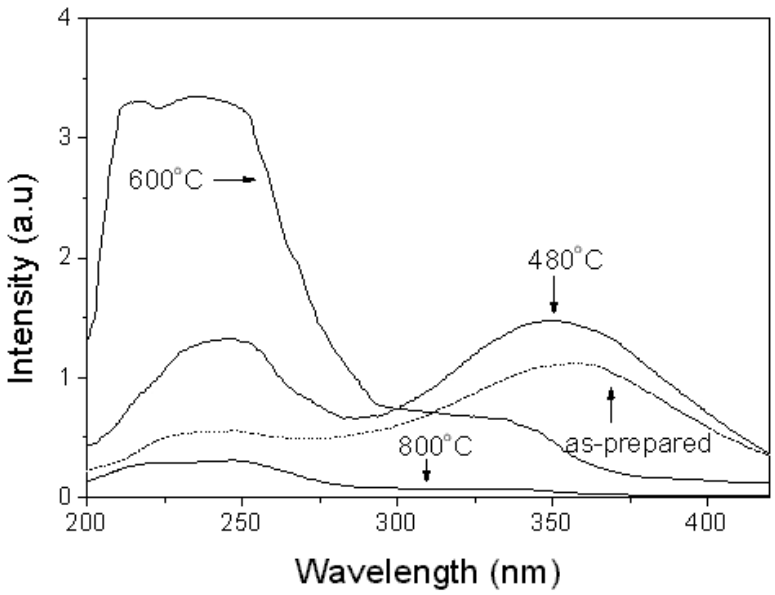

Figure 6. Excitation spectra for AAMs prepared in $C_2H_2O_4$ (sample A) after being annealed at different temperatures for 7 h. All the spectra were obtained under a monitoring wavelength of 420 nm.

and 204 (6.08 eV) nm, respectively. No absorption band at 294 nm was observed in the absorption spectra of sample B. This absorption band was believed to originate from $C_2O_4^{2-}$

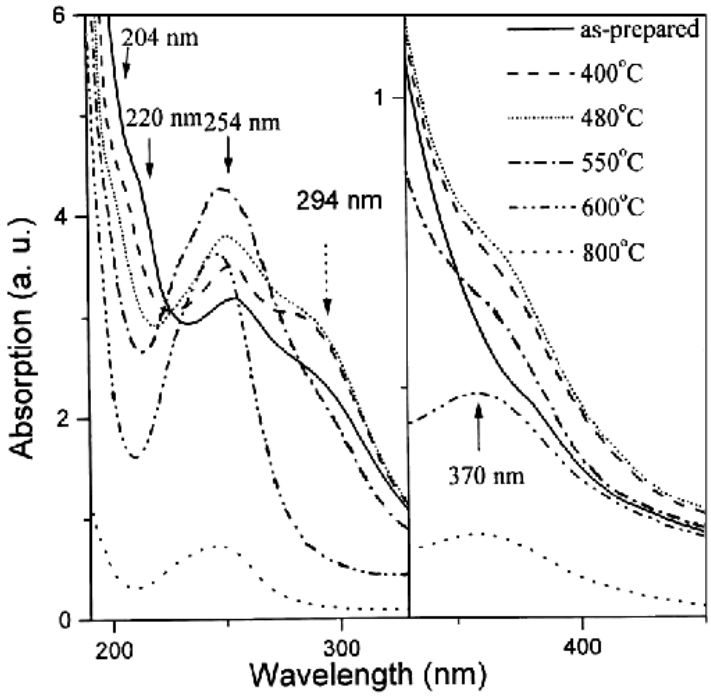

Figure 7. Absorption spectra for AAMs prepared in $C_2H_2O_4$ (sample A) after being annealed at different temperatures for 7 h.

involved during the anodization process to prepare the AAMs (XPS measurement shows the existence of $C_2O_4^{2-}$ in sample A). When annealing temperature $T \geqslant 550\,^{\circ}C$, the absorption band at 294 nm disappeared entirely, due to the heat-dissolution of the $C_2O_4^{2-}$ in AAMs. The absorption band at 294 nm will not be discussed in the following. With rising T, two phenomena are remarkable: (1) the intensities of the absorption bands at 370 nm and 254 nm increase first, reach a maximum (at 480 °C and 550 °C, respectively), then decrease; (2) all the absorption bands exhibit a shift to shorter wavelengths.

The results of EPR measurements for sample A are shown in figure 8. An obvious EPR signal with a g factor of 1.9765 appears in the EPR spectrum of as-prepared AAMs. This implies that there exist many F^+ centres in AAMs because other oxygen vacancies (F and F^{2+} centres) are not paramagnetic [7]. Investigation of the process of alumina growth can help us understand why the as-prepared AAMs contain many oxygen vacancies. As shown in figure 9, Al^{3+} combines with O^{2-} to produce Al_2O_3 at the Al_2O_3/Al interface. The Al atoms under positive potential are easy to oxidize to produce Al^{3+} (the voltage is not lower than 26 V and the electric field intensity is about 0.71 V nm^{-1} between the Al layer and the electrolyte). It can be deduced that the density of Al^{3+} is higher than that of the O^{2-} that infiltrates the alumina layer at the Al_2O_3/Al interface, which means that the Al atoms are oxidized under an oxygen scarce atmosphere. It is reported that heating Al_2O_3 under strongly reducing conditions results in producing oxygen vacancies [19, 20]. Therefore, our AAMs prepared under oxygen scarce atmosphere also contain many oxygen vacancies. Figure 8 also demonstrates that, with rising annealing temperature T, the density of F^+ centres in AAMs increases first, and then decreases. When $T = 800\,^{\circ}C$, our EPR device cannot detect the signal of F^+ centres.

Choi and Takeuchi [8] carried out a calculation of the electronic states of an ion cluster which simulates the F^+-type colour centre in Al_2O_3 crystals and predicted five possible optical

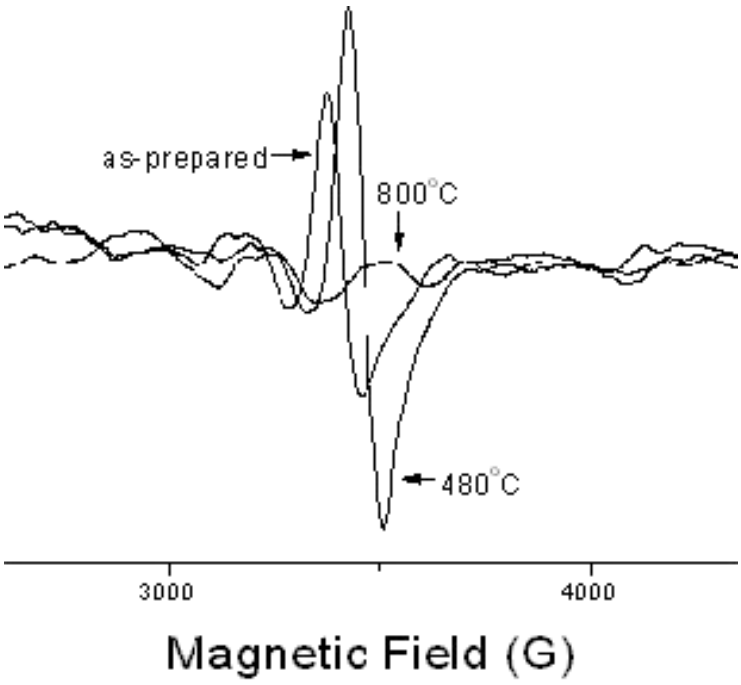

Figure 8. X-band EPR traces at room temperature for AAMs prepared in $C_2H_2O_4$ after being annealed at different temperatures for 7 h.

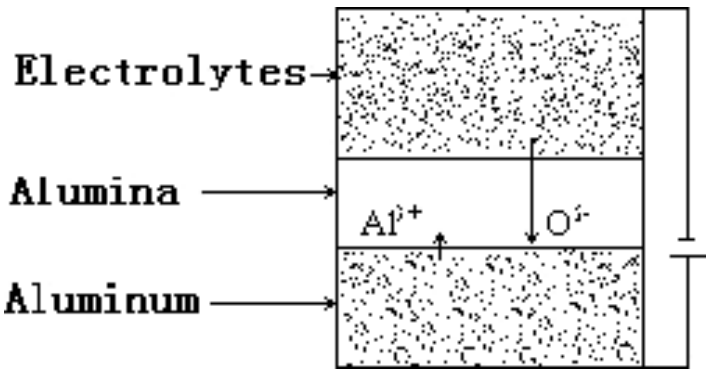

Figure 9. Schematic plot of the processes involved in AAM growth.

absorption transitions at 4.7, 5.5, 5.7, 6.0 and 6.1 eV. Harutunyan *et al* [9–12] have studied the VUV–UV absorption (and excitation) spectra of electron-irradiated (or neutron-irradiated) pure Al_2O_3 crystals. Their experiments revealed that the absorption bands at 4.86, 5.4 and 6.3 eV were attributed to the F^+ colour centre, and that the absorption band at 5.4 eV produced a blue emission band peaking around 3.0 eV (413 nm). Our experimental data concerning the absorption and PL peak positions for AAMs are basically consistent with the calculated [8] and observed [9–12] results: (1) excitation and emission band (5.28 eV–5.4 eV; 2.95 eV–3.0 eV); (2) absorption transitions (4.88 eV–4.7 eV, 5.64 eV–5.7 eV; 6.08 eV–6.1 eV). It should be noted that the positions of some absorption bands predicted by [8] (6.1 and 6.0 eV, 5.5 and 5.7 eV)

are too close to be distinguished experimentally. This agreement makes us believe that the optical properties of AAMs in the wavelength range of 200 nm to 500 nm depend on the F^+ centres in AAMs.

However, compared with the calculated [8] and observed [9–12] results, our experimental data exhibit two new features: (1) a 470 nm emission band; (2) a 360 nm excitation band (370 nm absorption band). It should be emphasized that our AAMs are amorphous, whereas the objects studied before [8–12] are crystals. This difference in structure may be responsible for the new optical features of our AAMs. It was suggested that when an ion (F^+ centre in the present case) is placed into a glass matrix, the local environment influences its energy levels, giving rise to the splitting of levels into several components which are shifted and broadened [23]. For the same reason, the influence of local environment around the F^+ centres in amorphous AAMs brings a new 370 nm (3.35 eV) energy level in.

With the increase of the annealing temperature, three factors affect the intensities of PL and absorption. (1) The remaining aluminium in AAM is oxidized under an oxygen-poor atmosphere, and it is possible that in the newly formed alumina there exist many oxygen vacancies, which increase the intensities of PL and optical absorption of F^+ centres. (2) The F^+ centres in AAMs combine with oxygen diffusing into the AAMs, which will lead to the decreases of F^+ centre density and the intensities of PL and optical absorption of F^+ centres. (3) AAMs are partly crystallized (see figure 2) and the structure distortion become less, which causes the electron densities at all energy levels to be redistributed. When annealing temperature $T \leqslant 480\,^\circ$C, the first factor is predominant, so the intensity of PL and absorption at all positions become stronger with rising T. With further increasing T ($480\,^\circ\text{C} < T \leqslant 600\,^\circ$C), the third factor plays an important role. Therefore the intensity of 470 nm emission with an excitation of 360 nm decreases dramatically, while that of 420 nm emission with an excitation of 235 nm increases continuously. When $T > 600\,^\circ$C, the second factor is predominant, hence the intensities of PL and optical absorption originating from F^+ centres become weaker with rising T.

With increasing T, the observed blue-shift of the peak positions of PL and optical absorption may originate from the release of internal stress of AAMs as suggested by Du [7]. The internal stress is established in AAMs by the volume expansion of aluminum during oxide formation [24], which will cause the band gap of the alumina to become narrow [25], and, hence, the spacing of the energy levels of the F^+ centres to decrease. This leads the PL band to present red-shifts in comparison with that of the AAMs without the remaining aluminium. With increasing temperature, the remaining aluminum is gradually oxidized to form alumina, resulting in the decrease of internal stress. After annealing at high temperature, the internal stress is released entirely, so there is not much difference between the samples annealed at $600\,^\circ$C and $800\,^\circ$C.

4. Conclusion

Anodic alumina membranes (AAMs) with highly ordered nanochannel arrays were prepared by anodizing aluminum in acid solutions. The photoluminescence (PL) emission spectra show a peak at 470 nm. The PL excitation spectra of AAMs consist of a broad band centred at 235 nm and a narrow band peaking around 360 nm under a monitoring wavelength of 470 nm. There are five prominent absorption bands (or edges) at 370, 294, 254, 220 and 204 nm in the absorption spectra of AAMs prepared in oxalic solutions. With the increase of the annealing temperature, the intensities of PL and absorption bands increase first, then decrease, and a blue-shift is found. The optical properties of AAMs in the wavelength range of 200 nm to 500 nm depend on F^+ centres in AAMs. The energy levels of F^+ centres in AAMs are split

and shifted, and a new energy level of 3.35 eV is brought in, due to the amorphous nature of AAMs.

Study of the optical properties of AAMs is important to the investigation of the mechanism of new properties that appear in the nanomaterials synthesized using AAMs as templates and offers a new way to explore the mechanism of the optical behaviours of crystal Al_2O_3. The AAMs exhibiting a blue PL band are expected to be useful in optical devices.

Acknowledgment

This work was supported by the Key Project of National Fundamental Research and the Natural Science Foundation of China (grant No 19974055).

References

[1] Martin C R 1994 *Science* **266** 1961
[2] Mausda H and Satoh M 1996 *Japan. J. Appl. Phys.* **35** 1126
[3] Yi G and Schwarzacher W 1999 *Appl. Phys. Lett.* **74** 1746
[4] Liu K, Chien C L, Searson P C and Zhang K Y 1998 *Appl. Phys. Lett.* **73** 1436
[5] Li J, Papadopoulos C, Xu J M and Mosdovits M 1999 *Appl. Phys. Lett.* **75** 367
[6] Li Y, Meng G W, Zhang L D and Phillipp F 2000 *Appl. Phys. Lett.* **76** 2011
[7] Du Y, Cai W L, Mo C M, Chen J, Zhang L D and Zhu X G 1999 *Appl. Phys. Lett.* **74** 2951
[8] Choi S and Takeuchi T 1983 *Phys. Rev. Lett.* **50** 1474
[9] Harutunyan V V, Gevorkyan V A, Grigoryan N E, Erisyan G N and Martirosyan U M 1988 *Sov. Phys.–Solid State* **30** 1332
[10] Harutunyan V V, Grigoryan N E, Gevorkyan V A and Erisyan G N 1989 *Nucl. Instrum. Methods* A **282** 622
[11] Harutunyan V V, Gevorkyan V A, Grigoryan N E and Erisyan G N 1990 *Phys. Status Solidi* b **160** k71
[12] Harutunyan V V, Gevorkyan V A and Grigoryan N E 1991 *Nucl. Instrum. Methods* A **308** 200
[13] Chen W, Tang H, Shi C, Deng J, Shi J, Zhou Y, Xia S, Wang Y and Yin S 1995 *Appl. Phys. Lett.* **67** 317
[14] Runeiman W A 1968 *Solid State Commun.* **6** 537
[15] Caulfield K J, Cooper R and Boas J F 1993 *Phys. Rev.* B **47** 55
[16] Evans B D and Stapelbroek M 1978 *Phys. Rev.* B **18** 7089
[17] Canut B, Benyagoub A, Marest G, Meftah A, Moncoffre N, Ramos S M M, Studer F, Thevnard P and Toulemonde M 1995 *Phys. Rev.* B **51** 12 194
[18] Kimura K, Kaneko J, Sharma S, Hong W and. Itoh N 1999 *Phys. Rev.* B **60** 12 626
[19] Lee K H and Crawford J H Jr 1978 *Appl. Phys. Lett.* **33** 273
[20] Lee K H and Crawford J H Jr 1979 *Phys. Rev.* B **19** 3217
[21] Moulton P F 1986 *J. Opt. Soc. Am.* B **3** 125
[22] Shimazu M 1993 *Photon. Spectra* **27** 131
[23] Patek K 1970 *Glass Lasers* (London: Iliffe)
[24] Jessensky O, Müller F and Gösele U 1998 *Appl. Phys. Lett.* **72** 1173
[25] Vassiliou J K, Mehrotra V. Russell M W, Giannelis E P. Michael R D, Shull R D and Ziolo R F 1993 *J. Appl. Phys.* **73** 5109